

POST-BUCKLING ANALYSIS OF PRESTRESSED CONCRETE  
BEAM-COLUMNS BY THE DISPLACEMENT CONTROL STRATEGY

變位制御法에 의한 프리스트레스트 콘크리트 보-기둥 構造의 後挫屈거동 해석

강 영 진\*

Kang, Young-Jin

요 약

유한요소법을 바탕으로 한 프리스트레스트 콘크리트 평면 보-기둥 구조의 後挫屈 거동에 대한 數値解析法을 제시하였다. 콘크리트의 균열, 變形軟化 및 PS강재의 항복과 같은 材料 非線形성을 고려하였다. 挫屈 거동 연구에 필수적 요소인 幾何學的 非線形성을 Updated Lagrangian Formulation에 의하여 고려하였다. 현재의 재료성질 및 변형상태에 부합하는 增分形 평형방정식을 수립하고 이것을 不平衡 荷重補正에 의한 Newton-Raphson 반복법으로 푼다. 좌굴후 발생하는 하중-변형 곡선의 下降部는 비선형 평형 방정식의 解法中 일반적으로 많이 사용되는 荷重 增分法이 아니라 變位增分法을 사용함으로써 올바르게 추적한다. 요소내의 재료성질 변화는 層積分法에 의하여 고려한다. 본 논문에서는 콘크리트 균열에 의한 中立軸이동의 영향을 정확히 고려하기 위하여 추가적으로 軸方向변위에 대한 內部自由度를 설정하였다. 본 논문에서 제안하는 방법의 정당성과 응용성을 나타내 보일 수 있는 數値解析 例題를 제시하였다.

ABSTRACT

A numerical procedure based on the finite element method for the post-buckling analysis of planar prestressed concrete beam-column structures is presented. Material nonlinearities such as the cracking, strain-softening and crushing of concrete and the yielding of prestressing steel are included. Geometric nonlinearity which is an essential factor in studying the post-buckling behavior is considered by the updated Lagrangian formulation. Incremental equilibrium equations which are valid for the current material properties and deformation are set up and solved by the Newton-Raphson iteration scheme with the unbalanced load correction. The unloading branch of the load-displacement curve after buckling has taken place is traced correctly by the displacement control strategy rather than the usual load control strategy for the solution of nonlinear equilibrium equations. Varied material properties within the frame element are considered by the layer integration scheme. In the present element formulation the shift of the neutral axis due to the concrete cracking is accurately accounted for by incorporating an additional internal degree of freedom for the axial displacement. Numerical examples are presented to demonstrate the validity and applicability of the proposed method.

\* 정회원, 서울대학교 토목공학과 부교수, 공학박사

● 1989. 9. 9 접수. 본 논문에 대한 토론을 1990. 6. 30까지 본 학회에 보내주시면 1990. 9월호에 그 결과를 게재해 드리겠습니다.

## INTRODUCTION

Prestressed concrete compression members usually act as beam-columns due to the continuity of concrete structures. The stability analysis of these structures is complicated due to a number of factors which include the material nonlinearity of constituent materials and geometric nonlinearity. When these structures exhibit strain-softening or snap-through the structure stiffness matrix at some point in the solution path is non-positive definite (Fig. 1). The conventional methods for solving the nonlinear equations with the load control strategy are not applicable without modification. This study presents a numerical method for tracing

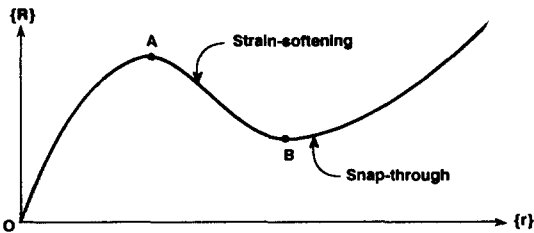


Fig. 1. Typical Load-Displacement Response for Structures with Non-positive Definite Stiffness Matrix

the post-buckling behavior of planar prestressed concrete beam-column structures based on the displacement control strategy. Nonlinear stress-strain relations for concrete and prestressing steel are incorporated, and varied material properties within frame elements are considered by the layer integration scheme.

## SOLUTION OF NON-POSITIVE DEFINITE SYSTEM OF EQUATIONS

Various schemes have been proposed in the past to circumvent the difficulties which arise in treating the non-positive definiteness of the structure stiffness matrix and passing over the limit point where the determinant of the stiffness matrix changes sign as at points A and B in Fig. 1. In the figure  $\{R\}$  represents the load vector and  $\{r\}$  represents the displacement vector.

Some of the numerical schemes will be reviewed to form the basis for the selection of a numerical scheme to be used in the present study.

### Imposed Displacement via the Change of Independent Variable

Argyris [1] first introduced this method and chose the displacement rather than the load as the independent variable. However, the loss of symmetry and the banded nature of the resulting stiffness matrix have placed some restrictions on its use.

### Augmenting the Stiffness Matrix

This method has been used by Whiteman et al [2] in solving frame type structures and later generalized by Sharifi [3] to handle shell structures. The method involves augmenting the structure with a set of linear generalized springs at each of the loaded joints so that the stiffness of the complete system, including the generalized springs, becomes positive definite. However, due to the coupling of all the loaded

degrees of freedom produced by the generalized spring system, the augmented stiffness matrix is generally a full matrix. The maximum increase in the solution time in solving the system of equations may be as much as 25% as shown by Sharifi[3]. The unbanded nature of the stiffness matrix may also cause numerical problems when the augmented spring stiffness is chosen to be too large in value. On the other hand, if the spring stiffness is chosen to be too small, it may have little effect on the resulting stiffness.

### Orthogonalizing Techniques

Bergan[4] developed an iterative scheme in which the iteration is carried out with variable load level. The idea is to adjust the external load so that the residual is always perpendicular to the external load. This should theoretically give the smallest residual in the least squares sense and hence converge quickly to the true solution. However, Powell et al[5] have found that the scheme does not produce consistent improvements in reliability and speed of convergence.

### Double Step Method

The solution at any instant is obtained in two steps by solving for the displacements  $\{r^u\}$  and  $\{r^e\}$  of two independent load conditions  $\{R^u\}$  and  $\{R^e\}$ . The final solution is obtained so that a certain constraint,  $\{C\} = \{0\}$  between the displacements  $\{r^u\}$  and  $\{r^e\}$ , is satisfied. In mathematical terms :

$$[K][\{r^u\} | \{r^e\}] = [\{R^u\} | \{R^e\}] \dots (1)$$

$$\{C(\{r^u\}, \alpha\{r^e\})\} = \{0\} \dots (2)$$

Equation(1) is used to solve for  $\{r^u\}$  and  $\{r^e\}$  and equation(2) is used to solve for the load factor  $\alpha$  so that the constraint equation  $\{C\} = \{0\}$  is satisfied. The matrix  $[K]$  can be non-positive definite, provided that it is not singular. In general,  $\{r^u\}$  is the displacement vector due to the unbalanced load  $\{R^u\}$ , and  $\{r^e\}$  is the displacement vector due to some reference external load  $\{R^e\}$ .

Bergan[6] uses two different methods of iteration depending on the sign of the determinant of the stiffness matrix : if no sign change is detected in two consecutive steps, conventional Newton-Raphson iteration is used ; when a sign change is detected in two consecutive steps, the direction of the external load increment is reversed. However, iteration is not performed to avoid numerical problems in the vicinity of the limit load where the stiffness matrix is nearly singular.

Powell and Simons[5] use the constraint condition :

$$r_n^u + \alpha r_n^e = \delta \dots (3)$$

for imposed deformation, where  $\delta$  is the prescribed displacement at the  $n^{\text{th}}$  degree of freedom. This method is identical with Batoz et al [7].

$$\{R^e\}^T[\{r^u\} + \alpha\{r^e\}] = 0 \dots (4)$$

corresponds to the iteration with constant work constraint. The imposed deformation of Powell et al[5] does not require the exact tangent stiffness to be formed, provided that the load is single valued in the displacement component  $n$ . This only involves a proper choice of the  $n^{\text{th}}$  displacement degree of freedom to be constrained. It has also been shown that an iteration with co-

nstant imposed deformation yields a more rapidly converged solution compared to the conventional iteration with constant load step. Because of the economy, speed of convergence and the versatility to handle various kinds of problems, this method is adopted for the numerical implementation of the present study.

**Description of the Present Numerical Formulation**

An automatic load generation based upon limiting the  $n^{\text{th}}$  imposed displacement increment  $\delta$  at the beginning of the displacement step is used. The constraint equations are :

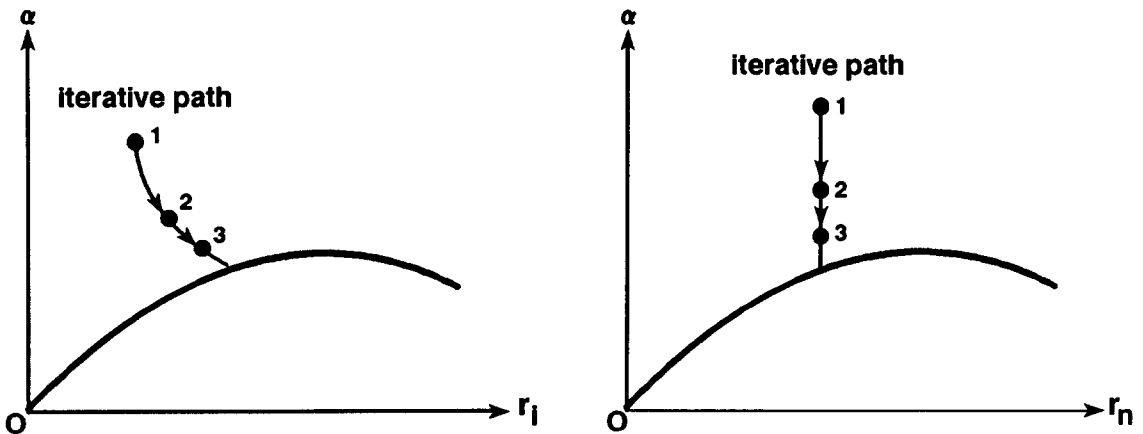
$$r_n^n + \alpha r_n^n = \delta \text{ for first iteration } \dots\dots\dots (5)$$

$$r_n^n + \alpha r_n^n = 0 \text{ for subsequent iterations}$$

The convergence criteria can be controlled either by the magnitude of the unbalanced load or the ratio of the displacement increments in successive iterations. The iterative path in the present solution scheme can be geometrically in-

terpreted as in Fig. 2. The method, when applied to a single degree of freedom system with linear material properties and undergoing a snap-through phenomenon, can be shown to converge on the first iteration.

In the present numerical formulation, path independent state determination, instead of path dependent state determination is carried out in each iteration for the current state determination; that is, the determination of element states such as strains, stresses, or deformations and stress resultants. This means that the state at the end of any iteration is found with reference to the beginning state, then discarded. The final state thus depends only on the beginning state and the sum of the displacement increments for all iterations, and is independent of the iteration path. As Powell and Simons [5] pointed out, the reason for adopting path independent state determination is that for the displacement control strategy the strains will frequently not increase progressively so that the path dependent scheme may incorrectly predict unloading.



(a) Load vs Displacement of the Unconstrained DOF (b) Load vs Displacement of the Constrained DOF

Fig. 2. Iterative Path for Imposed Displacement

Two kinds of convergence tolerances are used in this study; the displacement ratio tolerance and the maximum allowed unbalanced load. The displacement ratio tolerance is defined as the ratio of the displacement increment for the current iteration to the total displacement increment up to previous iteration of the current displacement step. The displacement component to be checked is the maximum translation or rotation occurring on the first iteration of the current displacement step. Between the translational and the rotational components of the displacement, the one which yields the greater ratio is the controlling displacement component. If the displacement ratio of this component is smaller than the displacement ratio tolerance the iteration for the current displacement step is stopped. Otherwise, the iteration continues. By setting appropriate value of the maximum allowed unbalanced load, excessive violation of equilibrium can be avoided. The ceiling on the number of iterations that can be carried out for each displacement step is also provided in case the above mentioned convergence criteria cannot be satisfied.

In the present study the convergence tolerance for changing the structure stiffness is provided so that either the constant stiffness or the variable stiffness iteration can be selected. If the displacement ratio is greater than this tolerance, then new structure tangent stiffness matrix is formed based on the current state and used for the next iteration. Otherwise, previously formed and reduced stiffness matrix is used again. The number of iterations required to arrive at the solution is affected by the value of this tolerance. In a typical nonlinear analysis problem the state determination phase takes up more computer time than the stiffness for-

mation and reduction phase. Thus, by using variable stiffness iteration the number of iterations required can be reduced, especially for ultimate load analyses in which the structure tangent stiffness varies steeply. However, for creep analyses in which the structure tangent stiffness stays essentially the same, constant stiffness iteration can be selected for economy.

### MODELING OF MATERIAL PROPERTIES

The stress-strain curves for the concrete and prestressing steel assumed in this study are shown in Fig. 3(a) and Fig. 3(b), respectively. The ascending portion of the concrete stress-strain curve is a parabola as originally proposed

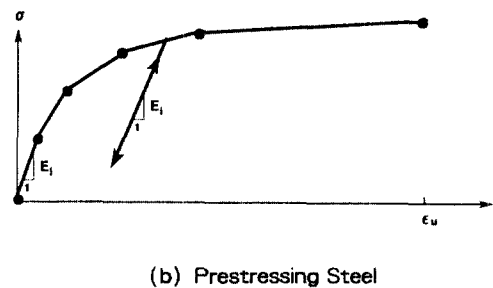
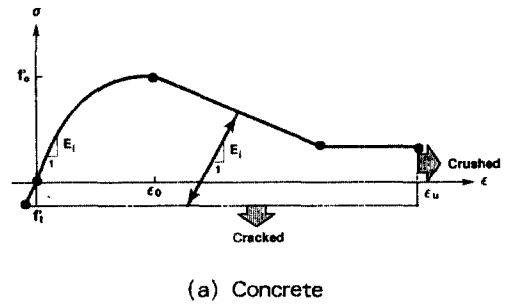


Fig. 3. Idealized Stress-strain Curves of Constituent Materials

by Hognestad[8]. The moduli for the descending and horizontal straight lines are assumed to be zero. The horizontal line portion of the curve is used for modeling the behaviour of the confined concrete. It is assumed that the concrete crushes when its compressive strain reaches the ultimate compressive strain, and cracks when its tensile stress reaches its tensile strength. Multilinear stress-strain curve is utilized for the prestressing steel in this study. Load reversal can be modeled for both the concrete and the prestressing steel.

### ELEMENT FORMULATION

A planar prestressed concrete frame can be idealized as an assemblage of planar prestressed concrete beam-column elements. Fig. 4 shows the beam-column element and its element degrees of freedom in local coordinates. Prestressing tendon is idealized as a straight truss element with constant axial force within the element. Its location in the element is defined by two end eccentricities  $e_i$  and  $e_j$ . It is assumed that perfect bond exists between the concrete and the prestressing steel.

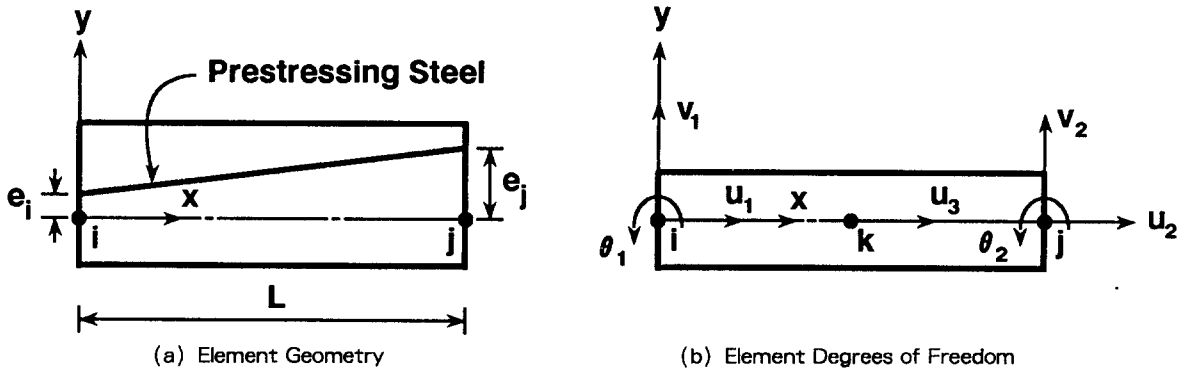


Fig. 4. Planar Prestressed Concrete Beam-column Element

The beam-column element is defined by its two end joints  $i$  and  $j$ , and an interior joint  $k$  which is located at the center of the element axis. Let  $u$ ,  $v$  and  $\theta$  be the  $x$ -displacement,  $y$ -displacement and the rotation of the joint, respectively. Then the joint displacement vector  $\{r\}$  of a beam-column element can be written as follows :

$$\{r\} = [u_1, u_2, u_3, v_1, v_2, \theta_1, \theta_2]^T \dots\dots(6)$$

Let  $u_0$  and  $v$  be the  $x$ -displacement and the  $y$ -displacement of an arbitrary point on the element axis.  $u_0$  and  $v$  are assumed to be para-

bolic and cubic functions of  $x$ , respectively. They can be expressed as functions of joint displacements as follows, with the nondimensional parameter  $p$  defined as  $p = x/L$  :

$$u_0(p) = (1-p)u_1 + pu_2 + 4p(1-p)u_3 \quad (7)$$

$$v(p) = (1-3p^2+2p^3)v_1 + (3p^2-2p^3)v_2 + L(p-2p^2+p^3)\theta_1 + L(-p^2+p^3)\theta_2 \dots\dots\dots(8)$$

While the shape function for the bending deformation is the usual Hermitian interpolation function, the function for the axial deformation is parabolic instead of the usual linear function. The reason for this is that by utilizing identical

linear variations of the axial strain for both bending and the axial deformations more accurate results are obtained for ultimate load analyses in which neutral axis of the element shifts due to the cracking of concrete. The internal degree of freedom  $u_3$  is condensed out statically in the element stiffness formulation phase, so that it is not included in the global joint degrees of freedom. Adopting Bernoulli-Navier's plane section hypothesis, the  $x$ -displacement  $u(x, y)$  and the axial strain  $\epsilon(x, y)$  of any point in the beam-column element can be written as follows :

$$u(x, y) = u_0(x) - y \frac{dv(x)}{dx} \dots\dots\dots (9)$$

$$\epsilon(x, y) = \frac{\partial u(x, y)}{\partial x} + \frac{1}{2} \left[ \frac{dv(x)}{dx} \right]^2 \dots\dots\dots (10)$$

The second term of the equation(10) represents the large displacement effect. It is assumed in this study that the strain is small even though the displacements and rotations may be large. Equation(10) expresses nonlinear strain-displacement relations and this is one of the sources of geometric nonlinearity. Another source is the fact that the equilibrium equations should be set up and solved based on the deformed configuration rather than the original underformed configuration as assumed in the linear analysis.

The incremental form of the strain-displacement relations at the current state can be derived from equations (6) to (10) as follows :

$$\Delta \epsilon = [B]\{\Delta r\} + \{\Delta r\}^T [C]^T [C]\{\Delta r\} / 2 \dots\dots\dots (11)$$

$$[B] = [-1/L, 1/L, 4(1-2p)/L, 6y(1-2p)/L^2, 6y(-1+2p)/L^2, 2y(2-3p)/L, 2y(1-$$

$$3p)/L] \dots\dots\dots (12)$$

$$[C] = [0, 0, 0, 6(-p+p^2)/L, 6(p-p^2)/L, (1-4p+3p^2), (-2p+3p^2)] \dots\dots\dots (13)$$

Applying the principle of virtual displacements the following form of the tangential equilibrium equations can be derived[9].

$$\{dR\} = [K_t]\{dr\} \dots\dots\dots (14)$$

$$[K_t] = [K_0] + [K_g] \dots\dots\dots (15)$$

$$[K_0] = \int_V [B]^T E_t [B] dV \dots\dots\dots (16)$$

$$[K_g] = \int_V [C]^T \sigma [C] dV \dots\dots\dots (17)$$

Equation(14) is the desired form of the tangential equilibrium equations which are valid for the current geometry and material properties. In equation(16)  $E_t$  is the tangent modulus of elasticity of the material at the current state. The tangent stiffness matrix  $[K_t]$  consists of the small displacement stiffness matrix  $[K_0]$  which includes the material nonlinearity and the geometric stiffness matrix  $[K_g]$  which represents the large displacement effects.

In order to account for the varied material properties within an element over the depth of the cross section, the cross section is divided into a discrete number of concrete layers and the layer integration is carried out for the calculation of the stiffness matrix and element stress resultants. The evaluation of  $[K_t]$  is performed at the center of each element since only a reasonably good estimate of the tangent stiffness matrix is required in solving nonlinear equilibrium equations by the iterative method with unbalanced load corrections. However, accurate evaluation of the internal resisting load is essential in the iterative scheme, thus they are computed by a three point Gaussian quadrature along the length of the beam-column

element combined with the layer integration over the depth of the element. The contribution of the prestressing steel segments is added directly treating them as one-dimensional truss elements.

The tangential equilibrium equations for the entire structure are assembled in the fixed global coordinate system from the contributions of all the elements in the structure by the direct stiffness analysis procedure. It is to be noted that the direction cosines of the displacement transformation matrix for each element are continuously changing according to the current orientation of the local element coordinate system.

#### NONLINEAR ANALYSIS PROCEDURE

After imposing appropriate boundary conditions, the assembled nonlinear equilibrium equations for the structure are solved by the displacement control strategy. Let the  $n^{\text{th}}$  degree of freedom  $r_n$  be the controlled displacement component. The imposed displacement is divided into a discrete number of displacement increments. For each displacement step the following iterative procedure is carried out. At the beginning of each step the unbalanced load vector,  $\{R^u\}$ , the external load vector,  $\{R^e\}$ , and the increment  $\delta$  of the controlled degree of freedom  $r_n$  are known.

(1) Form the tangent stiffness matrix for each element based on the current geometry and material properties. Assemble the structure tangent stiffness matrix  $[K_t]$  in global coordinates using the current displacement transformation matrix for each element.

(2) Solve  $[K_t]\{r^u\} = \{R^u\}$  and  $[K_t]\{r^e\} =$

$\{R^e\}$  for displacement increments  $\{r^u\}$  due to the unbalanced loads and the increments  $\{r^e\}$  due to the external loads in two separate analyses.

(3) Solve equation (5) for the load multiplier  $\alpha$  distinguishing the first and subsequent iterations. Then the increments of the displacement vector and the load vector for the current displacement step are  $\{r^u\} + \alpha\{r^e\}$  and  $\alpha\{R^e\}$ , respectively. Transform the global displacement increments into local coordinates to obtain element end displacement increments.

(4) Compute the strain increment by equation (11) and add to the previous total to obtain the current total strain. This is done for each Gaussian quadrature point and concrete layer.

(5) Add displacement increments to the previous total to get the current total joint displacements  $\{r\}$ . Update element geometry based on  $\{r\}$ , that is, update the element length and the displacement transformation matrix.

(6) Compute stresses by the nonlinear stress-strain law.

(7) Compute the element end forces by integrating current total stresses for each element in local coordinates. Transform them into global coordinates using displacement transformation matrices to assemble the internal resisting loads  $\{R^i\}$ .

(8) Subtract  $\{R^i\}$  from the current total external load vector to obtain the unbalanced load vector  $\{R^u\}$ .

(9) Go back to step (1).

Steps (1) to (9) are continued until the unbalanced loads  $\{R^u\}$  are within allowable tolerances and displacement ratio convergence tolerances are within prescribed limits as explained earlier. If all convergence requirements are satisfied the



analysis proceeds to the next displacement step.

## NUMERICAL EXAMPLES

A computer program based on the analysis procedure described above has been written. Two numerical examples solved by this program are presented to show the validity and applicability of the proposed procedure.

### SCHREYER-MASUR ARCH

Schreyer and Masur[10] presented analytical solutions for end clamped shallow circular

arches subjected to uniform pressure. This example is chosen to verify the present numerical procedure for solving a snap-through problem and tracing the post-buckling branch of the load-displacement curve. The structural geometry and material properties are shown in Fig. 5. 1. Due to the symmetry of the structure one half of the arch is modeled by 10 beam-column elements. The response of the structure is obtained by selecting the central deflection  $w$  as the controlled degree of freedom and imposing  $w = 7$  inches in 14 equal displacement steps of 0.5 inches each. Linearly elastic material properties are assumed.

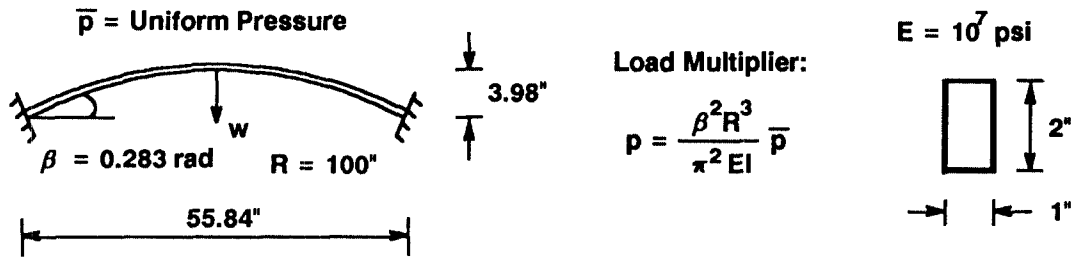


Fig. 5. 1 Schreyer-Masur Arch-Structure and Loading

The analysis has been carried out with the following convergence tolerances for each displacement step: displacement ratio =  $10^{-3}$ ; maximum unbalanced force =  $1^{\text{lb}}$ ; maximum unbalanced moment =  $10^{\text{inch-lbs}}$ . The average number of iterations for each displacement step is 3. The load-displacement response of the arch is shown in Fig. 5. 2. Good agreement between the theoretical solution and the present numerical solution can be noted. Relatively large discrepancy at the end of the load-deflection curve can be attributed to the unconservativeness of the pressure loading acting on the structural configuration which has been

altered significantly after the snap-through.

### Aroni Column

Aroni[11, 12] tested a series of eccentrically loaded pretensioned concrete columns to study their behavior under various conditions of eccentricity, slenderness, and the amount of prestress. He also presented an analytical procedure to predict the response on these columns based on the finite difference method. One of the columns, designated by  $D_240b3$ , which exhibits non-positive definite stiffness after buckling, is analyzed by the present method to

test the accuracy of the present nonlinear analysis procedure by the displacement control strategy. The 80-inch(2032-mm) long column was axially pretensioned with four 0.198<sup>in</sup>(5.03 mm) diameter high tensile strength steel wires. The prestress was released at 14 days after

casting of concrete, then the column was cured under water until 28 days after casting when the eccentric load with the eccentricity of 1.5<sup>in</sup> (38mm) was applied up to failure. Initial concrete compressive stress of 1.40<sup>ksi</sup>(9.62<sup>MPa</sup>) and the initial midspan deflection of 0.25<sup>in</sup>(6.35<sup>mm</sup>)

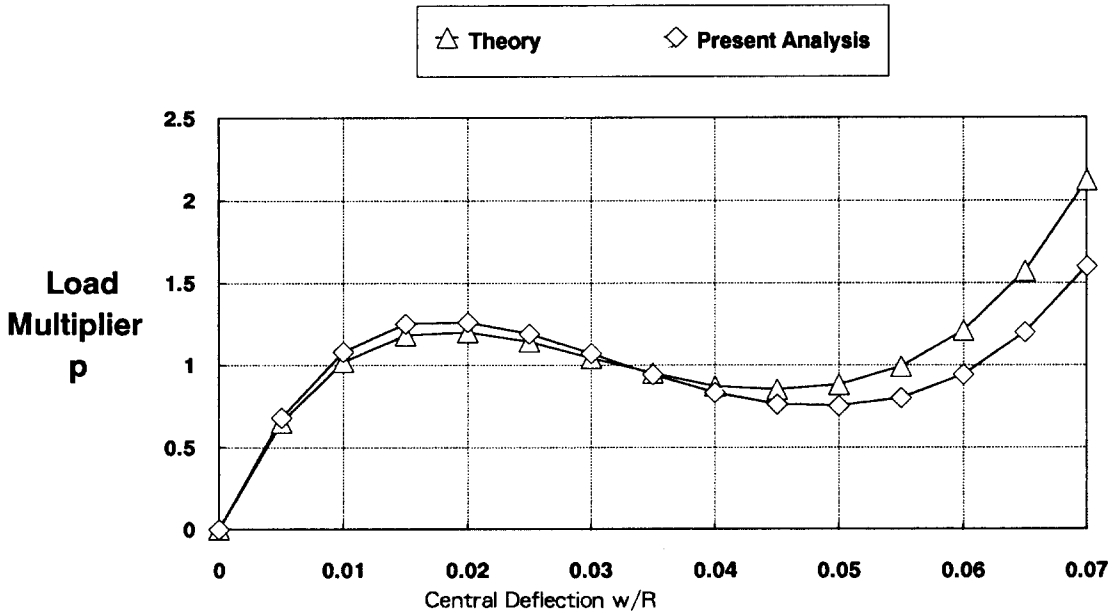


Fig. 5. 2 Schreyer – Masur Arch – Comparison of Central Deflections

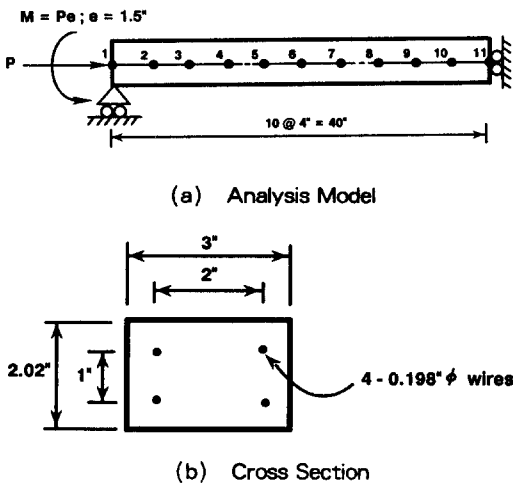


Fig. 6. 1 Aroni Column – Structure and Loading

was recorded in the experiment. Due to the symmetry of the structure and the loading, one half of the column is analyzed with 10 equal elements, and the cross section is divided into 10 concrete layers. The analysis model is shown in Fig. 6. 1. Concrete material properties are as follows : 28-day cylinder strength  $f'_c = 5.59\text{ksi}$  (38.5<sup>MPa</sup>) ; initial modulus of elasticity  $E_i = 4.94 \times 10^3\text{ksi}$  (23 $\times 10^3\text{MPa}$ ) ; modulus of rupture  $f'_t = 0.559\text{ksi}$  (3.85<sup>MPa</sup>) ; ultimate compressive strain = 0.006. The modulus of prestressing steel wires is  $29.3 \times 10^3\text{ksi}$  (20 $\times 10^3\text{MPa}$ ).

The response of the structure is obtained by selecting the midspan deflection  $\omega$  as the controlled degree of freedom and imposing  $w = 2.9$

inches in 11 displacement steps of varying size. The convergence tolerances used in the

sent numerical formulation traces the post-buckling response of the structure accurately.

## CONCLUSIONS

A numerical procedure, based on the finite element method for the material and geometric nonlinear analysis of planar prestressed concrete beam-column structures, has been presented. The solution of nonlinear equilibrium equations is carried out by the displacement control strategy rather than the usual load control strategy. The method has been shown to be capable of predicting the displacements, internal forces and reactions of these structure through their elastic, inelastic, buckling and post-buckling ranges in one complete analysis. The present modeling of material properties is capable of capturing dominant axial and flexural behavior of planar prestressed concrete beam-column structures. The shift of the neutral axis due to cracking of concrete is accurately accounted for in the present element formulation by incorporating additional internal degree of freedom for axial displacement. The accuracy and applicability of the present method has been demonstrated by numerical examples.

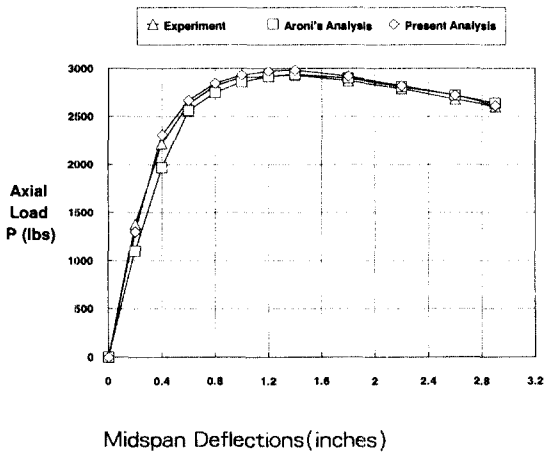


Fig. 6. 2 Aroni Column—Comparison of Load—Deflection Values

analysis for each displacement step is as follows : ratio of the displacement increment to the total displacement = 0.02 ; maximum unbalanced force = 10<sup>lbs</sup> ; maximum unbalanced moment = 100<sup>in-lbs</sup>. The average number of iterations for each displacement step is 6. 5.

The experimental and analytical results for the midspan deflection are plotted in Fig. 6. 2. Good agreement between the experimental and analytical results can be observed. Maximum load that the column can sustain before buckling is 2980<sup>lbs</sup>(13.3<sup>kN</sup>) for the present analysis, compared with 2930<sup>lbs</sup>(13.0<sup>kN</sup>) for the experiment. The figure also shows that the pre-

## ACKNOWLEDGMENTS

This study was conducted while the author was visiting the University of California, Berkeley in the United States of America from December 1987 through February 1989 as a Visiting Associate Research Engineer. Financial aid provided by the Korean Ministry of Education is gratefully acknowledged.

## REFERENCES

1. Argyris, J. H. , "Continua and Discontinua," Proceedings, First Conference on Matrix Methods in Structural Mechanics, Wright-Patterson Air Force Base, Ohio, 1965.
2. Whiteman, E. and Gaylord, E. H. , "Analysis of Unbalanced Multi-story Steel Rigid Frames," Proceedings of the American Society of Civil Engineers, May 1968.
3. Sharifi, P. , "Nonlinear Analysis of Sandwich Structures," Ph. D. Dissertation, Division of Structural Engineering and Structural Mechanics, University of California, Berkeley, 1971.
4. Bergan, P. , "Solution Algorithms for Nonlinear Structural Problems," Proceedings, International Conference on Engineering Applications of the Finite Element Method, Hovic, Norway, May 1979.
5. Powell, G. and Simons, J. , "Improved Iteration Strategy for Nonlinear Structures" International Journal for Numerical Methods in Engineering, Vol. 17, 1981.
6. Bergan, P. , "Solution Techniques for Nonlinear Finite Element Problems," International Journal for Numerical Methods in Engineering, Vol. 12, 1978.
7. Batoz, J. L. and Dhatt, G. , "Incremental Displacement Algorithms for Nonlinear Problems," International Journal for Numerical Methods in Engineering, Vol. 14, 1979.
8. Hognestad, E. , "A Study of Combined Bending and Axial Load in Reinforced Concrete Members," University of Illinois Engineering Experiment Station, Bulletin Series No. 399, Bulletin No. 1, 1951.
9. Kang, Y. J. and Scordelis, A. C. , "Nonlinear Analysis of Prestressed Concrete Frames," Journal of the Structural Division, Proceedings of the American Society of Civil Engineers, Vol. 106, No. ST2, 1980.
10. Schreyer, H. and Masur, E. , "Buckling of Shallow Arches," Journal of the Engineering Mechanics Division, Proceedings of the American Society of Civil Engineers, Vol. 92, No. EM4, 1966.
11. Aroni, S. , "Slender Prestressed Concrete Columns," UC-SESM Report No. 67-10, Division of Structural Engineering and Structural Mechanics, University of California, Berkeley, 1967.
12. Aroni, S. , "Slender Prestressed Concrete Columns," Journal of the Structural Division, Proceedings of the American Society of Civil Engineers, Vol. 94, No. ST4, 1968.